Indirect contributions to electron-impact ionization of Li^+ ($1s2s\ ^3S_1$) ions: Role of intermediate double-K-vacancy states

A. Müller,[1,*] A. Borovik Jr.,[2] K. Huber,[1] S. Schippers,[2] D. V. Fursa,[3] and I. Bray[3]
[1]*Institut für Atom- und Molekülphysik, Justus-Liebig-Universität Gießen, 35392 Giessen, Germany*
[2]*I. Physikalisches Institut, Justus-Liebig-Universität Gießen, 35392 Giessen, Germany*
[3]*Curtin Institute for Computation and Department of Physics, Astronomy and Medical Radiation Science, Curtin University, Perth, WA 6845, Australia*

(Received 27 November 2017; published 26 February 2018)

Fine details of the cross section for electron-impact ionization of metastable two-electron $Li^+(1s2s\ ^3S_1)$ ions are scrutinized by both experiment and theory. Beyond direct knockoff ionization, indirect ionization mechanisms proceeding via formation of intermediate double-K-vacancy (hollow) states either in a Li^+ ion or in a neutral lithium atom and subsequent emission of one or two electrons, respectively, can contribute to the net production of Li^{2+} ions. The partial cross sections for such contributions are less than 4% of the total single-ionization cross section. The characteristic steps, resonances, and interference phenomena in the indirect ionization contribution are measured with an experimental energy spread of less than 0.9 eV and with a statistical relative uncertainty of the order of 1.7%, requiring a level of statistical uncertainty in the total single-ionization cross section of better than 0.05%. The measurements are accompanied by convergent-close-coupling calculations performed on a fine energy grid. Theory and experiment are in remarkable agreement concerning the fine details of the ionization cross section. Comparison with previous R-matrix results is less favorable.

DOI: 10.1103/PhysRevA.97.022709

I. INTRODUCTION

Two-electron targets in photonic and electronic collisions are of special interest in atomic physics and astronomy. Their relative simplicity provides the best chance for theory to describe their structure and dynamics in atomic interactions with a good accuracy. Yet, two-electron systems are sufficiently complex to challenge the understanding of the most fundamental atomic processes such as ionization and excitation. Most work dealing with photon or electron interactions of two-electron systems has been performed on the helium atom in its ground level. By using crossed- and merged-beam techniques at small accelerators and ion storage rings [1], experiments with ionic heliumlike targets became feasible. In particular, measurements could be performed on Li^+ ions, which are the target of interest also in the present study. Results on $Li^+(1s^2)$ ions have been reported for electron-impact single and double ionization [2–7], single ionization and double excitation by photons [8], and recombination with free electrons [9].

Apart from the $1s^2\ ^1S$ ground state, also the excited states are of fundamental interest and play an important role in applications, mainly in plasma and astrophysics. However, providing well-characterized samples of excited atoms or ions for collision experiments is very difficult. Therefore, experimental knowledge about interactions of targets in excited states with any kind of projectile is very scarce. The best possibility for studying excited atoms or ions is to address metastable, that is, long-lived excited states. In He-like systems the $1s2s$ configuration supports metastable ^1S and ^3S levels. With its longer lifetime and increased statistical weight the ($1s2s\ ^3S$) level is more readily accessible to experiments than the associated ^1S level.

Early measurements on electron-impact ionization of $He(1s2s\ ^3S)$ were carried out by Dixon *et al.* [10], who determined absolute cross sections by using the crossed-beam technique. However, as theoretical methods for treating electronic collision processes evolved to high standards, a disturbing disagreement between theory and the experiment by Dixon *et al.* was uncovered by Fursa and Bray [11] using their convergent-close-coupling (CCC) approach. The discrepancy was repeatedly confirmed in a number of subsequent studies employing different theoretical methods. Part of the motivation for a previous experiment with Li^+ ions [6], in both the $1s^2\ ^1S$ ground and the metastable $1s2s\ ^3S$ levels, was the test of the CCC method to adequately describe electron-impact ionization of $Li^+(1s2s\ ^3S)$. Theory and experiment were found to be in good agreement. The long-standing discrepancy for $He(1s2s\ ^3S)$ has been brilliantly resolved in a recent experiment by Génévriez *et al.* [12], who convincingly demonstrate an underestimation of the uncertainties in the previous measurement.

While the results published on electron-impact ionization of metastable $He(1s2s\ ^3S)$ [10,12] and $Li^+(1s2s\ ^3S)$ [6] were focused on total single-ionization cross sections, an additional aspect was addressed in a detailed investigation of He-like $N^{5+}(1s2s\ ^3S)$ [13]. By scanning the electron-impact single-ionization cross section in fine steps with a good energy resolution and extremely good statistics, individual contributions to the measured total cross section could be identified. Amazingly good agreement was found between the measurements and CCC calculations carried out with very fine electron-energy steps. This approach is now also applied to electron-impact ionization of the $Li^+(1s2s\ ^3S)$ ion.

*alfred.mueller@iamp.physik.uni-giessen.de

The processes of interest are as follows.

(1) Direct (or knockoff) ionization (DI),

$$e^- + \mathrm{Li}^+(1s2s\ ^3S_1) \rightarrow \mathrm{Li}^{2+}(1s\ ^2S_{1/2}) + 2e^- \quad (1)$$

and

$$e^- + \mathrm{Li}^+(1s2s\ ^3S_1) \rightarrow \mathrm{Li}^{2+}(2s\ ^2S_{1/2}) + 2e^-, \quad (2)$$

with subsequent stabilization by photoemission.

(2) Indirect ionization proceeding via inner-shell excitation with subsequent autoionization (EA),

$$\begin{aligned} e^- + \mathrm{Li}^+(1s2s\ ^3S_1) &\rightarrow \mathrm{Li}^+(n\ell\, n'\ell') + e^- \\ &\downarrow \\ &\mathrm{Li}^{2+}(1s) + e^-, \end{aligned} \quad (3)$$

with $(n,n' \geqslant 2;\ \ell,\ell' = s,p,d,f,\dots)$.

(3) Indirect ionization involving resonant excitation, also termed dielectronic capture (DC) [1], as the first step in a process that finally ends with the production of Li^{2+}:

$$e^- + \mathrm{Li}^+(1s2s\ ^3S_1) \rightarrow \mathrm{Li}(2s\, n\ell\, n'\ell'), \quad (4)$$

with $(n,n' \geqslant 2;\ \ell,\ell' = s,p,d,f,\dots)$. The intermediate state formed by DC can decay by emission of two electrons. When the two electrons are simultaneously emitted by a double-Auger decay,

$$\mathrm{Li}(2s\, n\ell\, n'\ell') \rightarrow \mathrm{Li}^{2+}(1s) + 2e^-, \quad (5)$$

the whole process leading to the net production of Li^{2+} is termed resonant excitation auto–double ionization (READI). When the two electrons are emitted sequentially,

$$\begin{aligned} \mathrm{Li}(2s\, n\ell\, n'\ell') &\rightarrow \mathrm{Li}^+(n''\ell''\, n'''\ell''') + e^- \\ &\downarrow \\ &\mathrm{Li}^{2+}(1s) + e^-, \end{aligned} \quad (6)$$

with $(n'',n''' \geqslant 2;\ \ell'',\ell''' = s,p,d,f,\dots)$, the whole process also contributes to the net production of Li^{2+}. It is termed resonant excitation double autoionization (REDA).

The different ionization channels listed above cannot always be distinguished from one another. An example is the DI [Eq. (1)] and READI [Eq. (4) plus Eq. (5)] pair of reaction channels, which, starting from identical entrance channels, produce a Li^{2+} ion and two electrons sharing the available excess energy. No experiment can decide which mechanism is responsible for the exit channel. Similarly to a Young-type two-slit experiment, interference of the two indistinguishable reaction channels can occur. Hence, the shapes of READI resonances are distorted, and the interference effect leads to Fano line profiles [14]. Similar arguments hold for other combinations of reaction channels.

A subset of the intermediate configurations that can be produced from $\mathrm{Li}^+(1s2s\ ^3S_1)$ by DC, such as $2s^2n\ell$ $(n = 2,3,4,\dots,0;\ \ell = s,p,d,\dots)$, is found at energies below the $2s^2$ excitation threshold. The associated three-electron levels can stabilize by the emission of photons, but then only contribute to the electron-ion recombination channel. A single-Auger decay produces $1sn'\ell'$ configurations $(n' = 2,3,4,\dots;\ \ell' = s,p,d,\dots)$, which are nonautoionizing and, therefore, cannot contribute to the net single ionization of the Li^+ ion. Hence, the occurrence of REDA can be excluded for $2s^2n\ell$ DC resonances. If one finds such resonances in the cross section for the production of Li^{2+} from Li^+, the only possible reaction pathway responsible for their occurrence is the READI mechanism. Similar arguments hold for other intermediate configurations such as $2s2p^2$.

The dominant ionization channel in few-electron systems is DI followed by EA, by relative importance. READI, being based on a double-Auger decay, is a relatively small contribution. In more complex cases, however, indirect processes can provide the dominant contributions to the total single-ionization cross section. Examples are the electron-impact ionization of Fe^{15+} [15] and Xe^{24+} [16], where REDA resonances are responsible for a substantial enhancement of the total single-ionization cross section. The goal of the present study is to quantify the contributions of indirect ionization mechanisms to the cross section for electron-impact single ionization of metastable $\mathrm{Li}^+(1s2s\ ^3S_1)$ ions. All indirect pathways involve the production of hollow states of Li or Li^+, i.e., intermediate states with no electron residing in the K shell.

This paper is organized as follows. In Sec. II a brief description of the experimental technique and the measurements is given, and the convergent-close-coupling calculations performed in the present context are reported in Sec. III. In Sec. IV the experimental and theoretical results are presented and compared with one another. The R-matrix calculations of Berrington and Nakazaki [17] are included in the discussion. The paper ends with a Summary and Outlook, in Sec. V.

II. EXPERIMENT

The experimental setup and the procedures employed in the measurements have been described in detail previously [6,18–21]. In short, a beam of Li^+ ions was produced by using an electron-cyclotron-resonance ion source. In an oven inside the plasma chamber metallic Li was evaporated. The vapor entered the source plasma, where Li^+ ions were produced. The source was operated at a potential of +12 kV so that the extracted ions could be accelerated towards the electrically grounded beam pipe. After acceleration the ions were dispersed according to their charge and mass by a magnetic dipole sector field. An isotopically pure beam of 12 keV $^7Li^+$, containing a fraction $(1-\alpha)$ of ions in the $1s^2\ ^1S_0$ ground level and a fraction α of ions in the $1s2s\ ^3S_1$ metastable level, was selected by appropriately setting the magnetic sector-field strength. It is worth mentioning in this context that no significant fraction of metastable $\mathrm{Li}^+(1s2s\ ^1S_0)$ ions in the parent ion beam was detected in detailed energy scans around the associated ionization threshold [6].

The desired ions were transported by electrostatic beam-optical elements to a 90° spherical deflector, which cleaned the beam from products of charge-changing collisions in the residual gas and focused it into a collimator consisting of two sets of variable apertures about 18.5 cm apart. Typical beam sizes used in the present electron-energy scan measurements were 2×2 mm^2. Right behind the collimator the ions passed a dense ribbon-shaped electron beam [22] at an angle of 90°. The length of the electron-ion interaction region was about 60 mm, corresponding to the width of the ribbon electron beam. Typical ion currents were in the range 50 to 100 nA. Electron currents increased proportional to $E_e^{3/2}$ according to

space-charge-limited transport at electron energy E_e. At the EA threshold of $Li^+(1s2s\ ^3S_1)$, that is, at $E_e \approx 88$ eV, the electron current was near 12 mA.

Li^{2+} product ions were separated from the parent Li^+ ion beam by a second dipole magnet. The primary ion beam was collected in a Faraday cup appropriately positioned inside the magnet chamber, while the ionized ions were transported to a high-efficiency single-particle detector [23,24] behind an additional 180° out-of-plane spherical deflector. Product-ion count rates at the EA threshold varied between scans depending on the ion current I_{ion} actually achieved. At $I_{ion} =$ 80 nA, for example, the total Li^{2+} product-ion count rate was 21 500 s^{-1} including background of 9300 s^{-1}, mainly arising from electron-stripping collisions of parent Li^+ ions in the residual gas between the 90° electrostatic spherical deflector in front of the electron-ion interaction region and the second magnetic sector field.

For the fine scan of the cross section for single ionization of Li^+ ions, a step size of 0.12 eV was chosen to cover the electron-ion collision energy range 69 to 119 eV. The number of counts accumulated at $E_e = 88$ eV was 5.8 million, resulting in a statistical relative uncertainty of the associated ionization cross section of about 0.05%. After background subtraction, the fine scan was normalized to the electron and ion currents using an estimated beam-overlap form factor that was obtained by averaging numerous previous crossed-beam measurements and is uncertain by up to 50%. The scan measurement, thus normalized, provides a preliminary, approximate, energy-dependent cross-section function. This approximate cross-section function was then normalized to discrete individual absolute measurements [6] obtained by properly considering the beam overlap. The animated-beam method [21,25] was used for determination of the absolute cross sections. For normalization to the absolute data the measured scan cross sections were multiplied by a smooth, almost-linear function of energy. Corrections to the approximate scan data of no more than 20% were required.

The total relative uncertainty of the measured absolute cross sections for single ionization by electron impact amounts to 15% [6]. The energy axis was calibrated to the known threshold energy, 75.64 eV, of ground-state Li^+ ions. The remaining uncertainty is estimated to be 0.3 eV in the investigated energy range.

III. CCC THEORY

We use the electron-atom scattering CCC theory initially developed for quasi-one-electron targets [26–28] and then extended to quasi-two-electron targets [11,29,30]. The CCC method has also been extended to positron and positive ion projectiles and molecular tagets [31,32].

In the present case we have a two-electron singly charged ion, Li^+, in either the ground or the metastable initial state. The extraordinary precision of the experiment allows the observation of the DI, EA, REDA, and READI processes contributing to electron-impact single ionization. Accordingly, the CCC calculations must incorporate these processes by allowing the residual electron to be left in an excited state of $Li^{2+}(n\ell)$. So as to make the calculations tractable we restrict $1 \leqslant n \leqslant 3$ with $0 \leqslant \ell \leqslant n-1$. The remaining electron is described using diagonalization of Li^{2+} in a Laguerre basis of $N_0 = 30$, with $N_l = N_0 - \ell$ and $\ell \leqslant 3$, and exponential fall-off parameter $\lambda = 2$. Such a diagonalization provides a good description of the negative-energy (one-electron) states but generates too many positive high-energy states, which are of no interest to us here. In making two-electron configurations we keep only $N_l = 25 - \ell$ of the obtained one-electron orbitals. Diagonalization of the two-electron Li^+ Hamiltonian leads to a total of 407 states consisting of 54 ^1S, 52 $^1P^o$, 1 $^1P^e$, 51 $^1D^e$, 2 $^1D^o$, 46 $^1F^o$, 48 $^3P^o$, 4 $^3P^e$, 52 $^3D^e$, 48 $^3D^e$, 2 $^3D^o$, 1 $^3F^e$, and 46 $^3F^o$ terms.

The energies of the lowest-lying discrete states are accurate to within a few percent, with the largest error being in the ground state. This is expected just as for He, where short-ranged functions for the "inner" electron are necessary to improve the accuracy of the ground state. Here we need to use the true longer-ranged eigenstates of Li^{2+} to ensure clear identifiable final ionization-plus-excitation states of Li^+. Consequently the single-ionization threshold of $Li^+(1^1S)$ turns out to be too low by approximately 1 eV: 74.546 eV rather than the experimental 75.640 eV [33]. A slightly lower ionization threshold has the systematic effect of leading to a slightly larger total ionization cross section.

Just as for He, the excited states of Li^+ are much easier to describe accurately. We find the $Li^+(2\ ^3S)$ threshold to be 16.586 eV, compared with the experimental value of 16.619 eV [33]. As our interest is far away from the $Li^+(1\ ^1S)$ threshold we consider the calculated structure to be sufficiently accurate.

Once the target description has been obtained, the most time-consuming part, performing the close-coupling calculations, begins. The CCC calculations have been performed on a fine incident-electron-energy mesh in order to resolve the structures seen in the experiment. The structures arise from the lower partial waves of the total orbital angular momenta, and so these require denser energy meshes. In all, the calculations were done separately for partial-wave total orbital angular momenta from 0 to 20. The contribution of partial waves to infinity was estimated using the Born subtraction technique [28].

IV. RESULTS

Figure 1 shows the cross sections for electron-impact single ionization of $Li^+(1s2s\ ^3S_1)$ and $Li^+(1s^2\ ^1S_0)$ ions resulting from the present CCC calculations. Because of the low ionization potential of the metastable Li^+ ion the cross section is relatively large. The threshold energy is 16.586 eV resulting from the present calculations versus 16.619 eV provided in the NIST level database [33]. The cross section reaches almost 4×10^{-17} cm^2 at its maximum and shows some fine features at energies of approximately 90 ± 20 eV. These features are the main topic of the present paper. They are associated with indirect ionization contributions to net total single ionization of the metastable Li^+ ion by electron impact.

The cross section for the Li^+ ground level is very noticeably smaller than that for the metastable Li^+ ion. The ionization threshold obtained in the CCC calculations is 74.546 eV, which is lower by around 1 eV than the 75.640-eV threshold given by NIST [33]. The cross section is dominated by far by the DI mechanism [see Eq. (1)]. Very small features that result

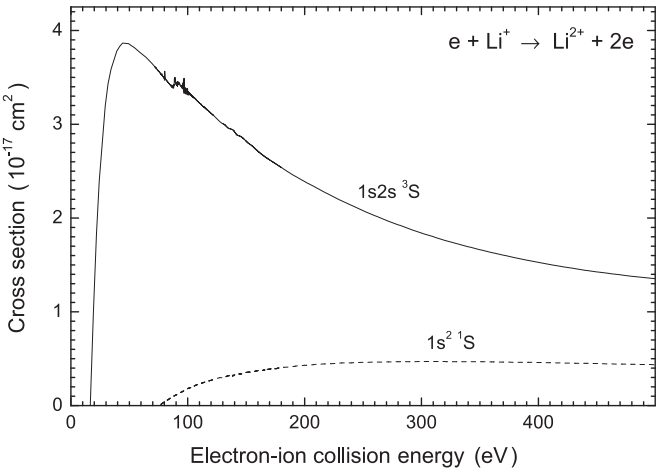

FIG. 1. Cross sections for electron-impact single ionization of $Li^+(1s2s\ ^3S_1)$ (solid line) and $Li^+(1s^2\ ^1S_0)$ (dashed line) calculated using the CCC method and applying an extremely fine energy mesh.

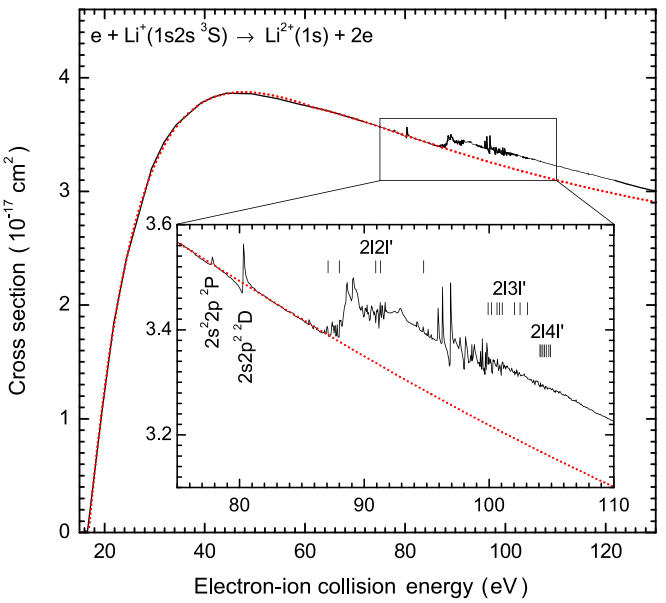

FIG. 2. Detail of the cross section for the metastable $Li^+(1s2s\ ^3S_1)$ ion displayed in Fig. 1. Inset: Further expansion of the energy region around the *K*-shell excitation threshold, which is at about 88 eV. Vertical bars indicate energies of doubly excited terms in the Li^+ ion relative to $Li^+(1s2s\ ^3S_1)$. They are based on measurements by Diehl *et al.* [34] from which the excitation energy of the metastable parent ions has been subtracted. The dotted red line is a fit to the cross section from its threshold to the onset of indirect ionization features. The fit is based on a formula suggested by Younger [35] for the representation of electron-impact direct-ionization cross sections. It has been extrapolated to energies beyond the *K*-shell excitation threshold. The two READI resonance features that can be unambiguously identified are indicated by the associated terms.

from direct and resonant inner-shell double excitation and subsequent Auger decays [5] are not visible at the level of detail that can be displayed in the overview of the cross section. Thus, the cross section for ground-level Li^+ should be and apparently is a smooth function of the energy as expected for DI.

For better visualization of the fine details in the ionization of the metastable Li^+ ion, Fig. 2 zooms in on the energy range of the cross-section maximum and slightly beyond. The inset in the figure is a further expansion of details and is focused on the region of the *K*-shell excitation threshold, which is at about 88 eV. At this level of magnification, details of the features caused by indirect ionization mechanisms become visible. There are step features and resonances which are due to the EA, READI, and REDA mechanisms, respectively, listed in Eqs. (3)–(6). The most prominent step feature is located at the EA threshold, where $2s^2$ and $2s2p$ states can be excited. In order to obtain a suitable representation of the fine excursions of the cross section from a smooth curve as expected for the DI mechanism alone, a very fine mesh of calculations was necessary. Results were obtained for more than 2000 energies which were concentrated in the region of present interest. Usually, about 10 to 20 energies are sufficient to describe direct-ionization cross sections over a very wide energy range from threshold to far beyond the maximum with a good accuracy.

Figure 2 includes a dotted red line, which was obtained from a smooth-curve fit to the calculated cross section for metastable $Li^+(1s2s\ ^3S_1)$ at energies below the EA threshold and excluding the visible resonance features. The smooth curve is meant to represent the DI contribution to the total single-ionization cross section. At the selected energies this cross section is exclusively due to the DI mechanism. The function behind the fit is a four-parameter formula suggested by Younger [35] for the representation of DI cross sections. He used this formula to fit his DI calculations obtained at a relatively small number of discrete energies and to interpolate the calculated results. In the present case the fit is used to extrapolate the DI cross section to the range where indirect ionization mechanisms come into play. Naturally, extrapolation to higher energies is associated with increasing uncertainty. However, in the energy range 90–120 eV relevant to the present study we estimate the maximum uncertainty of the extrapolated DI cross section to be no more than 1%.

As mentioned in Sec. I, the different electron-removal mechanisms present in the total single ionization cannot always be distinguished from one another. As a consequence the associated reaction channels can interfere and the cross section is not just the mere sum of individual contributions. Therefore, a unified treatment of single ionization is required including all reaction mechanisms and their mutual interactions at once. The independent-processes–isolated-resonances treatment of the problem is only an approximation that cannot be generally applied. The present CCC method is based on a unified treatment of ionization processes and as such it cannot provide an isolated cross section for direct ionization. In fact, in a situation where different ionization mechanisms are possible, the notion of isolated DI is meaningless because DI cannot generally be distinguished, e.g., from READI. An example for interference of READI and DI is visible in the inset in Fig. 2 at energies around 81 eV. The asymmetric resonance at 81 eV can be attributed to the READI mechanism populating an intermediate $Li^+(2s2p^2\ ^2D)$ term, which decays by a double-Auger process emitting two electrons simultaneously. Interference with DI produces the excursion of the cross section

TABLE I. Comparison of READI resonance parameters obtained from the present CCC calculations with the *R*-matrix results of Berrington and Nakazaki [17], both for electron-impact ionization of metastable Li^+ ions and for precision experiments [36,37] studying photoexcitation of neutral lithium by high-resolution Auger spectroscopy. Experimental energies are relative to the $Li^+(1s2s\ ^3S_1)$ level and were determined from the published data by considering the Li^+ excitation energies $E(1s^2\ ^1S_0 \rightarrow 1s2s\ ^3S_1) = 59.021$ eV and $E(1s^22s\ ^2S \rightarrow 1s^22p\ ^2P = 1.848$ eV [33] as well as the ionization energy $E = 5.392$ eV of neutral lithium [33]. E_e is the electron energy, Γ the apparent natural width, q the Fano asymmetry parameter, and A the amplitude parameter. Numbers in parentheses provide the uncertainties of the last digits of the experimental data.

Level	Data origin	E_e (eV)	Γ (meV)	q	A (Mb eV)
$2s^22p\ ^2P$	Present CCC	77.80	124	3.08	0.030
	[17]	77.87	129	4.74	0.038
	[36]	77.87(3)	118(3)	—	—
$2s2p^2\ ^2D$	Present CCC	80.30	97	1.97	0.118
	[17]	80.41	97	1.44	0.105
	[37]	80.36(5)	103(10)	—	—

below the undisturbed DI cross section (represented by the dotted line) just before the peak of the resonance is reached.

Usually, interference effects in electron-impact single-ionization cross sections are small and this is also the case in the present example. Therefore, the introduction of an overall DI cross-section contribution can be useful because it helps to assess the effects of the additional indirect ionization mechanisms. The DI cross section would result if the indirect ionization mechanisms could be switched off. When applying such a concept one has to keep in mind that the effects of interference can make the total cross section including DI, EA, REDA, and READI smaller than the straight DI cross section.

It is interesting to note that the present CCC results and the *R*-matrix calculations by Berrington and Nakazaki [17], also based on unified close-coupling theory, show very similar results for the $Li^+(2s^22p\ ^2P)$ and $Li^+(2s2p^2\ ^2D)$ READI resonances. From the calculated energy dependences the resonance parameters can be extracted from both treatments. Moreover, the resonance energies and apparent natural widths of the two doublets can be compared with precision experiments using narrow-bandwidth synchrotron radiation [36,37]. The numbers are provided in Table I.

Considering the READI resonance energies and the ionization thresholds calculated for the ground and metastable level of Li^+ one can state that deviations of the present CCC energies from accurate experimental results (with 0.03- to 0.05-eV uncertainties for the triply excited terms in neutral Li) are less than 0.1 eV. It is reasonable therefore to identify the additional features in the calculated cross section on the basis of measured level energies. The inset in Fig. 2 shows three sets of vertical bars, which represent the excitation energies of $2\ell2\ell'$, $2\ell3\ell'$, and $2\ell4\ell'$ terms derived from high-resolution Auger spectroscopy after photoabsorption by neutral Li [34]. The onset of EA at about 87 eV is associated with the $2s^2\ ^1S$ doubly excited level. The biggest EA step, at approximately 88 eV, can be assigned to the threshold for $2s2p\ ^3P^o$ excitation. At an energy almost 3 eV higher, that is, at about 91 eV, the

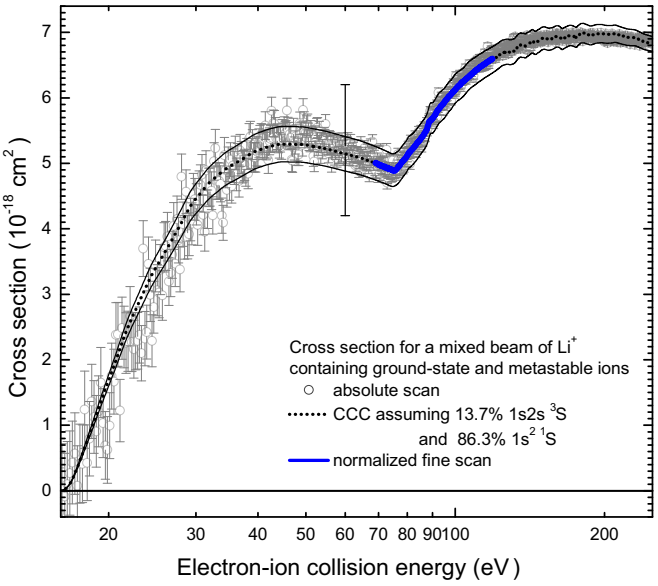

FIG. 3. Apparent cross sections for a mixed beam of Li^+ ions containing $1s^2\ ^1S_0$ ground-state and $1s2s\ ^3S_1$ metastable ions. Absolute previous cross-section data [6] with statistical error bars are shown in gray. A representative total-error bar is provided for the data point at 60 eV. The present densely spaced data points obtained from a fine energy scan appear as a thick solid blue line. Results of a CCC model cross section for a mixed ensemble of parent Li^+ ions assuming fractions of 13.7% metastable and 86.3% ground-level ions are represented by the dotted black line. Thin solid lines represent alternative CCC models with 13%–87% and 14.4%–85.6% mixtures of metastable and ground-level Li^+ ions.

$2p^2\ ^1D^e$ and the $2s2p\ ^1P^o$ terms are populated, causing the second largest EA step in the cross section. The relatively pronounced resonance features at energies between 96 and 97 eV must be associated with three-electron levels within Rydberg series converging to $2\ell3\ell'$ doubly excited states and are most likely due to $2\ell3\ell'3\ell''$ configurations.

Figure 3 shows an overview of the experimental data on electron-impact ionization of Li^+ ions in comparison with CCC model calculations. Throughout this paper cross sections are shown as a function of the electron-ion collision energy, that is, the relative energy in the center-of-mass system of the incident electron and the target ion. The measurements were carried out with a lithium ion beam containing a mixture of ions in the ground level and ions in the $1s2s\ ^3S_1$ metastable level. The experimental conditions were the same as those for "experiment 1" described in the previous publication by Borovik *et al.* [6]. Accordingly, Fig. 3 reports the previous cross sections on an absolute scale (open gray circles with statistical error bars) to which the present scan measurement was normalized. The densely spaced, fine-scan, filled blue data points appear as a thick solid line in the energy range 69 to 119 eV. The typical absolute uncertainty of the experimental cross sections is indicated by the solid black error bars shown for the data point at 60 eV. This comprises a systematic uncertainty of 6.3%, an energy-dependent uncertainty of the electron current transported through the interaction region decreasing from 7% at 69 eV to 5.4% at 119 eV, and a statistical uncertainty (4.8%

at 60 eV) which is relatively high because of the substantial background. All uncertainties were added in quadrature to determine the total error bars, which are of the order of 15%. In contrast to these numbers, the statistical uncertainty of the present scan measurement is only about 0.05%.

In order to simulate the experiment, an assumption about the fraction α of metastable ions in the parent ion beam has to be made. Since the experiment does not provide the fractions they have to be inferred from comparison with theory. From the present CCC calculations $\alpha = 0.137$ [and $(1-\alpha) = 0.863$ for ground-level Li^+] is found to give the best agreement with the experiment. The model CCC calculation based on these fractions is shown in Fig. 3 by the line consisting of black dots. Alternatively, the figure shows two theoretical models as thin solid lines based on the CCC calculations from Fig. 1 with 13.0%–87.0% and 14.4%–85.6% fractions of metastable and ground-level ions, respectively. All theory curves were convoluted with a 0.9-eV full width at half-maximum (FWHM) Gaussian to simulate the experimental energy spread. The comparison with the measured cross-section data demonstrates the sensitivity, by which the fractions are determined for a given set of theoretical results. A question at this point is, of course, the accuracy of the calculated cross sections.

In the publication by Borovik *et al.* [6] a fraction of 13% metastable ions had been inferred from the previous CCC calculation, which comprised a basis of 256 states. The present calculations were much more extensive and comprise up to 407 states. The new extended cross-section calculations for ground-level Li^+ ions are about 1% to, at most, 2% above the previous results except for the threshold region, where slightly different ionization potentials cause large relative deviations. For metastable $Li^+(1s2s\ ^3S_1)$ the new cross sections are about 5% to 6% above the previous results. These differences explain why different fractions of metastable and ground-level ions were obtained. One has to conclude that the previous CCC calculations for the metastable ions were not completely converged yet.

The CCC calculations represented by thin solid lines in Fig. 3 show a number of gentle oscillations in the model cross sections. Closer inspection reveals that these oscillations are associated with the cross section for ground-level Li^+ ions. The periods of these unphysical oscillations are of the order of 10 eV and their amplitudes are at the level of 1% of the electron-impact single-ionization cross section. The origin is attributed to expected pseudoresonances that depend on the basis set used in the CCC calculations. For further analysis of the present experiment, the oscillations in the cross section for ground-level Li^+ ions were avoided by replacing the CCC result with a smooth fit function of the type suggested by Younger [35] for the representation of DI cross sections.

Figure 4 presents the present electron-energy scan measurement of the apparent cross section for a mixed beam of $Li^+(1s^2\ ^1S_0)$ and $Li^+(1s2s\ ^3S_1)$ ions. Even at this level of magnification the individual data points cannot be distinguished from one another and appear as a thick solid blue line. At energies below 75.6 eV, which is the threshold energy for ionization of the ground-level component in the ion beam, the cross section is only due to ionization of the metastable fraction. As discussed in the context of Fig. 2 the only contribution to the cross section of metastable $Li^+(1s2s\ ^3S_1)$

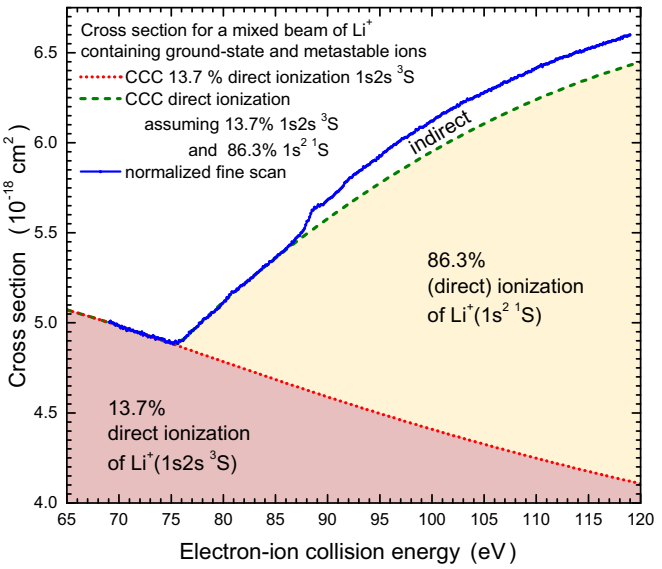

FIG. 4. The present fine-scan electron-impact single-ionization cross section for Li^+ ions is represented by densely spaced, small filled blue circles. The dotted red line with dark shading is 0.137 times the DI cross section of metastable $Li^+(1s2s\ ^3S_1)$ inferred from the CCC result (see Fig. 2). The dashed olive-green line is the sum of DI cross sections inferred from the CCC calculations for assumed fractions of 13.7% $Li^+(1s2s\ ^3S_1)$ and 86.3% $Li^+(1s^2\ ^1S_0)$. The lightly shaded area represents the DI of the 86.3% ground-level fraction of the Li^+ parent ion beam. The remaining white area under the scan cross-section curve is due to indirect ionization processes of the metastable fraction of the parent Li^+ ions.

at energies below 75 eV is from the DI channel. The DI contribution to the electron-impact ionization of metastable $Li^+(1s2s\ ^3S_1)$ is shown as the dotted red line in Fig. 2. This contribution multiplied by $\alpha = 0.137$ matches the present scan measurement at energies below 75.6 eV. The reduction factor 0.137 is required since an assumed fraction of 13.7% metastable $Li^+(1s2s\ ^3S_1)$ ions was present in the parent Li^+ beam. The 13.7% $Li^+(1s2s\ ^3S_1)$ DI contribution to the mixed-beam cross section is shown by the dotted red line in Fig. 4.

At energies above 75.6 eV, ionization of ground-level Li^+ adds to the apparent cross section. As explained above, the cross section for electron-impact ionization of $Li^+(1s^2\ ^1S_0)$ is almost exclusively due to DI. In order to avoid problems with ripples and with numerical instabilities in the calculated cross section, the CCC result was fitted by a smooth Younger-type function as described above. The resulting smooth function was multiplied by a factor 0.863 to account for the assumed 86.3% fraction of $Li^+(1s^2\ ^1S_0)$ ions in the parent ion beam and then added to the 13.7% $Li^+(1s2s\ ^3S_1)$ DI contribution. The resulting sum curve is shown as the dashed olive-green line in Fig. 4. The measured scan cross section deviates from the DI sum curve because it includes the effects of indirect ionization channels, EA, READI, and REDA, on the ionization of $Li^+(1s2s\ ^3S_1)$ ions present in the parent ion beam. The related excess area under the measured cross section is labeled "indirect" in Fig. 4.

To best highlight the indirect ionization effects on the cross section for $Li^+(1s2s\ ^3S_1)$ ions, the DI contributions represented

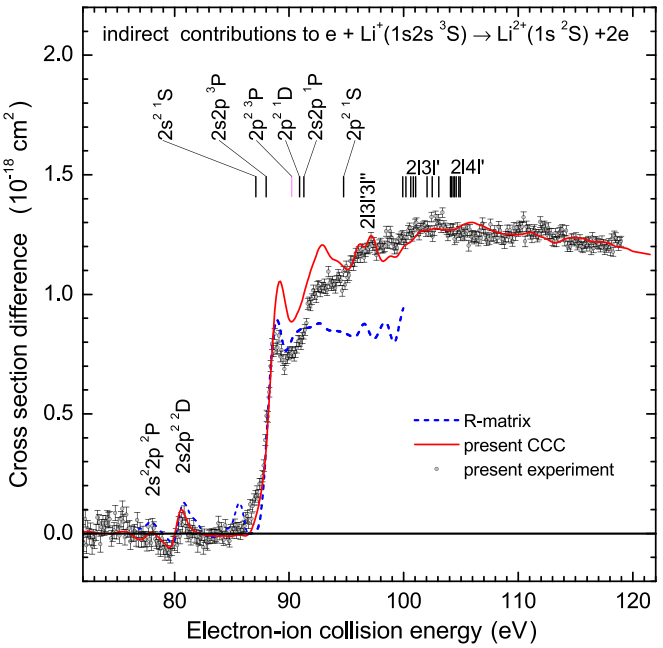

FIG. 5. Part of the total electron-impact single-ionization cross section of (100%) $Li^+(1s2s\ ^3S_1)$ ions that is due to the effects of indirect ionization mechanisms. Data points with statistical error bars result after subtraction of the total DI contribution to the ionization of a mixed beam of ground-state and metastable Li^+ ions (dashed line in Fig. 4) from the experimental scan data (small filled blue circles in Fig. 4) and dividing the difference by 0.137. The solid red line represents the related result of the present CCC calculation (see text). The dashed blue line shows the associated result obtained from *R*-matrix calculations published by Berrington and Nakazaki [17]. The terms and configurations given in the figure show where contributions associated with such intermediate excited states are expected. In particular, the excitation energies of doubly excited states identified experimentally by Diehl *et al.* [34] are shown by the vertical black bars, which are also presented in Fig. 2. In addition, the theoretically expected energy of the $2p^2\ ^3P$ term [34] is indicated by the thin vertical magenta bar.

by the dashed olive-green line in Fig. 4 were subtracted from the measured scan data. The resulting difference was divided by $\alpha = 0.137$ so as to obtain the indirect ionization cross section for (100%) metastable $Li^+(1s2s\ ^3S_1)$ ions which is displayed in Fig. 5. Considering the effects of destructive interference of indirect and direct ionization channels it is better to speak of the cross-section difference rather than the indirect ionization cross section. The difference can become negative, and it apparently does at around 79.5 eV, while a cross section can only be $\geqslant 0$. The measured data clearly show the $2s2p^2\ ^2D$ READI resonance and an indication of the much smaller $2s^22p\ ^2P$ structure. The most pronounced feature is the sharp rise in the cross-section difference at about 88 eV, which is mainly due to the $1s2s\ ^3S \rightarrow 2s2p\ ^3P$ excitation threshold. The excitation onsets producing EA steps in the scan measurement can be assigned to the doubly excited levels observed in the high-precision photoexcitation and Auger spectroscopy experiment by Diehl *et al.* [34].

The next threshold found in the experimental cross section between 91 and 92 eV is much less pronounced. It can be associated with $1s2s\ ^3S \rightarrow 2p^2\ ^3P$ (not provided as an experimental result by Diehl *et al.* [34] but theoretically expected at about 90.3 eV), $1s2s\ ^3S \rightarrow 2p^2\ ^1D$, and $1s2s\ ^3S \rightarrow 2s2p\ ^1P$ excitations. A further EA step at about 94.7 eV is obvious in the experimental spectrum. It can be associated with $1s2s\ ^3S \rightarrow 2p^2\ ^1S$ excitation. Part of the cross-section increase in this energy region is probably caused by the presence of resonances belonging to $2\ell3\ell'3\ell''$ configurations. The last, gradual increase in the measured cross section, at around 100 eV, may be attributed to EA steps to $2\ell3\ell'$ configurations. Effects of higher-lying excited states on the scan spectrum are not obvious. The peak feature at approximately 89 eV is most likely caused by $2\ell2\ell'2\ell''$ REDA resonances attached to the higher-lying doubly excited $2\ell2\ell'$ levels. Auger cascades via the $2s^2\ ^1S$ and the $2s2p\ ^3P$ autoionizing levels are possible for those resonances.

Along with the experimental data, two theoretical results for the effects of indirect ionization processes are displayed in Fig. 5. The present CCC calculation is shown in Figs. 1 and 2 and the present indirect ionization spectrum was obtained by subtracting the dotted red line shown in Fig. 2 from the calculated cross section for metastable $Li^+(1s2s\ ^3S_1)$. The solid red line in Fig. 5 resulted after convolution with a 0.9-eV FWHM Gaussian. Apart from deviations in the energy range 88.5 to 95 eV the CCC results are in very good agreement with the experimental spectrum. Even the $2s2p^2\ ^2D$ READI resonance seen in the experiment is perfectly well reproduced by theory, although this mechanism involves capture of the incident electron by the metastable Li^+ ion with simultaneous excitation of the *K*-shell electron and a subsequent three-electron Auger decay in which one electron falls into the *K* shell and two other electrons leave the intermediate atom simultaneously. Given the strength of theory in describing this mechanism correctly it is a little surprising to see the deviations just above the strongest EA threshold. The discrepancy appears to be due to an overestimation of the contributions arising from $2\ell2\ell'n\ell''$ READI/REDA resonances which are located below the $2\ell2\ell'$ doubly excited levels to which an $n\ell''$ electron is attached.

However, the deviations occurring just above the steep rise in the EA contribution are in the range of per mille of the single-ionization cross section. True convergence in the CCC calculations for two-electron targets can only be established by using complete expansions for both electrons. Such expansions would also yield a double-ionization cross section. However, such expansions are not practical due to their immense computational requirements. Here we have used two-electron configurations with a complete expansion for one electron and just a few discrete orbitals for the other. This has allowed us to treat some of the doubly excited states, which is not possible in the frozen-core (2*s* only) model. Due to the rapid growth in the size of the calculations with an increasing number of "core" orbitals, a systematic convergence study of this topic has not been attempted. Though the outstanding agreement with experiment is very encouraging and validates the multicore approach, it cannot be expected to be perfect. Furthermore, the resultant double-ionization cross section arising in such calculations is 0. We also note that in the CCC theory ionization is associated with excitation of any open positive-energy state. The decay path that the state may take has no bearing on the results. Optical decay of intermediate autoionizing levels

cannot be excluded but can safely be neglected for low-Z atoms and ions such as Li and Li^+, with $Z = 3$.

The second theoretical curve results from the R-matrix calculations carried out by Berrington and Nakazaki [17]. Their cross section for the electron-impact ionization of $Li^+(1s2s\ ^3S_1)$ is approximately 20% above the present CCC calculations. By fitting a smooth Younger-type curve [35] to their cross section at energies lower than 75 eV the DI part of the cross section was determined. After subtraction of this DI contribution from the total single-ionization cross section and convolution with a 0.9-eV FWHM Gaussian, the dashed blue line in Fig. 5 is obtained. It is slightly below but still very close to the present experiment. The $2s2p^2\ ^2D$ READI resonance is also quite well reproduced. However, the R-matrix calculations predict further READI resonances at about 85.7 eV which are present neither in the experiment nor in the CCC calculation. This is reminiscent of an effect that had been observed previously in R-matrix calculations for electron-impact ionization of lithiumlike parent ions such as C^{3+} [38] and O^{5+} [39]. The problem is in a limited set of basis states that does not allow one to describe all possible decay channels of triply excited levels such as $2\ell n'\ell' n''\ell''$ when n' and n'' are high. The basis set used by Berrington and Nakazaki [17] did not include $1sn\ell$ configurations with $n \geqslant 4$. Hence they could not describe single-Auger decay of resonances with configurations such as $2\ell 2\ell' 4\ell''$, which are most likely to decay by a single-Auger process to $1s4\ell$ states which cannot contribute to net single ionization. Because of this deficiency, the strengths of READI resonances can be vastly overestimated. This is probably also the case for the ionization of $Li^+(1s2s\ ^3S_1)$ ions.

There is yet another problem with the R-matrix result in the context of Fig. 5. Since the calculated cross section is about 20% above the present CCC result one would have to conclude on the basis of the R-matrix calculation that the fraction of metastable $Li^+(1s2s\ ^3S_1)$ ions in the parent beam of the experiment was about 11.4%. By normalization to 100% metastable ions the experimental cross-section difference would become larger by a factor of 1.2 and thus exceed the R-matrix result by about 60% at an electron-ion collision energy of 100 eV. This means that the effect of indirect ionization processes in the total single-ionization cross section is substantially underestimated by the R-matrix calculation at energies above the lowest EA threshold.

V. SUMMARY AND OUTLOOK

With only two bound electrons, helium atoms and heliumlike ions are among the simplest targets in electronic and photonic interactions. When both electrons reside in the K shell indirect single-ionization mechanisms require double excitations, which may be accompanied by the capture of the incident electron. As a consequence, the effects of indirect ionization channels are very small and direct knockoff ionization by far prevails. Metastable helium atoms or heliumlike ions are the simplest atomic systems, with two electrons occupying two different shells. A single excitation of the K-shell electron is sufficient to produce an autoionizing state which can contribute to net single ionization by a single-Auger decay. Hence the effects of indirect ionization channels are greatly enhanced in comparison to those of ground-level atoms and ions. Nevertheless, indirect ionization of $Li^+(1s2s\ ^3S_1)$ ions makes up for only a few percent of the total ionization cross section.

Differently from neutral helium, beams of only metastable ions cannot be produced with intensities sufficient for clean interacting-beam experiments. Therefore, studying the small contributions of indirect ionization of metastable He-like ions, which are only of the order of one-tenth the intensity available in an ion beam, is a challenge. Meaningful quantitative assessment of the effects of indirect ionization mechanisms requires a very high level of statistical quality of the measurements. Reaching such a level is complicated by the presence of about nine-tenths ground-state ions in the available beam. These ions do not contribute to the signal of the investigated indirect processes but produce "background" of direct ionization. In addition, there is real background arising from collisions in the residual gas of the experimental beam line. Stripping off the excited electron in the residual gas is easy, and hence stripping backgrounds are relatively high.

In the present experiment, a strong effort has been made to reduce the statistical uncertainty of the signal arising from electron-impact single ionization of metastable heliumlike $Li^+(1s2s\ ^3S_1)$ ions. A level of 0.05% statistical uncertainty could be accomplished with an electron energy spread of less than 0.9 eV in the energy region of interest. At this level of statistics fine details of the total ionization cross section arising from partly quite exotic indirect ionization channels could be revealed, and quantitative information about relative sizes of indirect ionization mechanisms could be extracted.

The level of detail required to quantify the relatively small contributions of indirect ionization mechanisms also poses a challenge to theory. By using large basis sets of states in a close-coupling treatment and by densely spacing the energies at which cross sections were calculated, the present CCC computations succeeded in explaining almost all features of the experimental cross section. Berrington and Nakazaki, in their paper on ionization of Li^+ ions of almost 20 years ago, wrote about convergent close coupling and other methods that "these methods have not been formulated so far for indirect ionization (nor indeed for photoionization) and therefore do not actually converge to the correct total ionization cross section when such effects are significant" [17]. In contrast to this statement, the present study demonstrates the superior potential of the CCC method for study of indirect ionization and for production of high-quality results, at least for a two-electron system.

It will be interesting to study ionization of heliumlike ions in the $1s2s\ ^3S_1$ level along this very fundamental isoelectronic sequence. Further work on this topic is under way.

ACKNOWLEDGMENTS

Support from Deutsche Forschungsgemeinschaft under Projects No. Mu 1068/13, No. Mu 1068/14, No. Mu 1068/20, and No. Mu 1068/22 is gratefully acknowledged. We thank Prof. S. Nakazaki for providing the numerical data obtained from the R-matrix calculations. D.V.F. and I.B. acknowledge the support of the Australian Research Council, the National Computer Infrastructure, and the Pawsey Supercomputer Centre.

[1] A. Müller, Adv. At. Mol. Opt. Phys. **55**, 293 (2008).
[2] W. C. Lineberger, J. W. Hooper, and E. W. McDaniel, Phys. Rev. **141**, 151 (1966).
[3] J. B. Wareing and K. T. Dolder, Proc. Phys. Soc. **91**, 887 (1967).
[4] B. Peart and K. T. Dolder, J. Phys. B **1**, 872 (1968).
[5] A. Müller, G. Hofmann, B. Weissbecker, M. Stenke, K. Tinschert, M. Wagner, and E. Salzborn, Phys. Rev. Lett. **63**, 758 (1989).
[6] A. Borovik Jr., A. Müller, S. Schippers, I. Bray, and D. V. Fursa, J. Phys. B **42**, 025203 (2009).
[7] B. Peart and K. T. Dolder, J. Phys. B **2**, 1169 (1969).
[8] S. W. J. Scully, I. Álvarez, C. Cisneros, E. D. Emmons, M. F. Gharaibeh, D. Leitner, M. S. Lubell, A. Müller, R. A. Phaneuf, R. Püttner, A. S. Schlachter, S. Schippers, and B. M. McLaughlin, J. Phys. B **39**, 3957 (2006).
[9] A. A. Saghiri, J. Linkemann, M. Schmitt, D. Schwalm, A. Wolf, T. Bartsch, A. Hoffknecht, A. Müller, W. G. Graham, A. D. Price, N. R. Badnell, T. W. Gorczyca, and J. A. Tanis, Phys. Rev. A **60**, R3350 (1999).
[10] A. J. Dixon, M. F. A. Harrison, and A. C. H. Smith, J. Phys. B **9**, 2617 (1976).
[11] D. V. Fursa and I. Bray, J. Phys. B **30**, 757 (1997).
[12] M. Génévriez, J. J. Jureta, P. Defrance, and X. Urbain, Phys. Rev. A **96**, 010701(R) (2017).
[13] A. Müller, A. Borovik Jr., K. Huber, S. Schippers, D. V. Fursa, and I. Bray, Phys. Rev. A **90**, 010701(R) (2014).
[14] U. Fano, Phys. Rev. **124**, 1866 (1961).
[15] J. Linkemann, A. Müller, J. Kenntner, D. Habs, D. Schwalm, A. Wolf, N. R. Badnell, and M. S. Pindzola, Phys. Rev. Lett. **74**, 4173 (1995).
[16] P. Liu, J. Zeng, A. Borovik Jr., S. Schippers, and A. Müller, Phys. Rev. A **92**, 012701 (2015).
[17] K. Berrington and S. Nakazaki, J. Phys. B **31**, 313 (1998).
[18] A. Borovik Jr., B. Ebinger, D. Schury, S. Schippers, and A. Müller, Phys. Rev. A **93**, 012708 (2016).
[19] J. Jacobi, H. Knopp, S. Schippers, A. Müller, S. D. Loch, M. Witthoeft, M. S. Pindzola, and C. P. Ballance, Phys. Rev. A **70**, 042717 (2004).
[20] A. Müller, K. Tinschert, C. Achenbach, R. Becker, and E. Salzborn, Nucl. Instrum. Methods B **10**, 204 (1985).
[21] A. Müller, K. Huber, K. Tinschert, R. Becker, and E. Salzborn, J. Phys. B **18**, 2993 (1985).
[22] R. Becker, A. Müller, C. Achenbach, K. Tinschert, and E. Salzborn, Nucl. Instrum. Methods B **9**, 385 (1985).
[23] J. Fricke, A. Müller, and E. Salzborn, Nucl. Instrum. Methods **175**, 379 (1980).
[24] K. Rinn, A. Müller, H. Eichenauer, and E. Salzborn, Rev. Sci. Instrum. **53**, 829 (1982).
[25] P. Defrance, F. Brouillard, W. Claeys, and G. Van Wassenhove, J. Phys. B **14**, 103 (1981).
[26] I. Bray and A. T. Stelbovics, Phys. Rev. A **46**, 6995 (1992).
[27] I. Bray, Phys. Rev. A **49**, 1066 (1994).
[28] I. Bray and A. T. Stelbovics, Adv. At. Mol. Opt. Phys. **35**, 209 (1995).
[29] D. V. Fursa and I. Bray, Phys. Rev. A **52**, 1279 (1995).
[30] D. V. Fursa and I. Bray, J. Phys. B **30**, 5895 (1997).
[31] A. S. Kadyrov and I. Bray, J. Phys. B **49**, 222002 (2016).
[32] I. Bray, I. B. Abdurakhmanov, J. J. Bailey, A. W. Bray, D. V. Fursa, A. S. Kadyrov, C. M. Rawlins, J. S. Savage, A. T. Stelbovics, and M. C. Zammit, J. Phys. B **50**, 202001 (2017).
[33] A. E. Kramida, Yu. Ralchenko, J. Reader, and NIST ASD Team (2017), *NIST Atomic Spectra Database (Version 5.5.1.)* (National Institute of Standards and Technology, Gaithersburg, MD, 2017), available at http://physics.nist.gov/asd.
[34] S. Diehl, D. Cubaynes, J.-M. Bizau, F. J. Wuilleumier, E. T. Kennedy, J.-P. Mosnier, and T. J. Morgan, J. Phys. B **32**, 4193 (1999).
[35] S. M. Younger, J. Quant. Spectrosc. Radiat. Transfer **26**, 329 (1981).
[36] S. Diehl, D. Cubaynes, J.-M. Bizau, L. Journel, B. Rouvellou, S. Al Moussalami, F. J. Wuilleumier, E. T. Kennedy, N. Berrah, C. Blancard, T. J. Morgan, J. Bozek, A. S. Schlachter, L. VoKy, P. Faucher, and A. Hibbert, Phys. Rev. Lett. **76**, 3915 (1996).
[37] D. Cubaynes, S. Diehl, L. Journel, B. Rouvellou, J.-M. Bizau, S. Al Moussalami, F. J. Wuilleumier, N. Berrah, L. VoKy, P. Faucher, A. Hibbert, C. Blancard, E. Kennedy, T. J. Morgan, J. Bozek, and A. S. Schlachter, Phys. Rev. Lett. **77**, 2194 (1996).
[38] H. Teng, H. Knopp, S. Ricz, S. Schippers, K. A. Berrington, and A. Müller, Phys. Rev. A **61**, 060704 (2000).
[39] A. Müller, H. Teng, G. Hofmann, R. A. Phaneuf, and E. Salzborn, Phys. Rev. A **62**, 062720 (2000).